

CMSSM with Yukawa Quasi-Unification Revisited

N. Karagiannakis,^{1,*} G. Lazarides,^{1,†} and C. Pallis^{2,‡}

¹*Physics Division, School of Technology, Aristotle University of Thessaloniki, Thessaloniki 54124, Greece*

²*Department of Physics, University of Cyprus, P.O. Box 20537, CY-1678 Nicosia, CYPRUS*

(Dated: September 20, 2011)

The constrained minimal supersymmetric standard model with $\mu > 0$ supplemented by an ‘asymptotic’ Yukawa coupling quasi-unification condition, which allows an acceptable b -quark mass, is reinvestigated. Imposing updated constraints from the cold dark matter abundance in the universe, B physics, the muon anomalous magnetic moment, and the mass m_h of the lightest neutral CP-even Higgs boson, we find that the allowed parameter space is quite limited but not unnaturally small with the cold dark matter abundance suppressed only via neutralino-stau coannihilations. The lightest neutralino with mass in the range (341 – 677) GeV is possibly detectable in the future direct cold dark matter searches via its spin-independent cross section with nucleon. In the allowed parameter space of the model, we obtain $m_h = (117 - 122.2)$ GeV.

PACS numbers: 12.10.Kt, 12.60.Jv, 95.35.+d

I. INTRODUCTION

The well-known *constrained minimal supersymmetric standard model* (CMSSM) [1–4], which is a highly predictive version of the *minimal supersymmetric standard model* (MSSM) based on universal boundary conditions for the soft *supersymmetry* (SUSY) breaking parameters, can be further restricted by being embedded in a SUSY *grand unified theory* (GUT) with a gauge group containing $SU(4)_c$ and $SU(2)_R$. This can lead [5] to ‘asymptotic’ *Yukawa unification* (YU) [6], i.e. the exact unification of the third generation Yukawa coupling constants h_t , h_b , and h_τ of the top quark, the bottom quark, and the tau lepton, respectively, at the SUSY GUT scale M_{GUT} . The simplest GUT gauge group which contains both $SU(4)_c$ and $SU(2)_R$ is the *Pati-Salam* (PS) group $G_{\text{PS}} = SU(4)_c \times SU(2)_L \times SU(2)_R$ [7, 8] – for YU within $SO(10)$, see Refs. [9, 10].

However, given the experimental values of the top-quark and tau-lepton masses (which, combined with YU, naturally restrict $\tan \beta \sim 50$), the CMSSM supplemented by the assumption of YU yields unacceptable values of the b -quark mass m_b for both signs of the parameter μ . This is due to the presence of sizable SUSY corrections [11] to m_b (about 20%), which arise [11, 12] from sbottom-gluino (mainly) and stop-chargino loops and have the sign of μ – with the standard sign convention of Ref. [13]. The predicted tree-level $m_b(M_Z)$, which turns out to be close to the upper edge of its 95% *confidence level* (c.l.) experimental range receives, for $\mu > 0$ [$\mu < 0$], large positive [negative] corrections which drive it well above [a little below] the allowed range. Consequently, for both signs of μ , YU leads to an unacceptable $m_b(M_Z)$ with the $\mu < 0$ case being much less disfavored.

The usual strategy to resolve this discrepancy is the introduction of several kinds of nonuniversalities in the scalar [9, 10] and/or gaugino [14, 15] sector of MSSM with an approximate preservation of YU. On the contrary, in Ref. [16], concrete SUSY GUT models based on the PS gauge group are constructed which naturally yield a moderate deviation from exact YU and, thus, can allow acceptable values of the b -quark mass for both signs of μ within the CMSSM. In particular, the Higgs sector of the simplest PS model [7, 8] is extended so that the electroweak Higgs fields are not exclusively contained in a $SU(2)_L \times SU(2)_R$ bidoublet superfield but receive subdominant contributions from other representations too. As a consequence, a moderate violation of YU is naturally obtained, which can allow an acceptable b -quark mass even with universal boundary conditions. It is also remarkable that the resulting extended SUSY PS models support new successful versions [17] of hybrid inflation based solely on renormalizable superpotential terms.

These models provide us with a set of ‘asymptotic’ Yukawa quasi-unification conditions which replace exact YU. However, applying one of these conditions in the $\mu < 0$ case does not lead [18, 19] to a viable scheme. This is due to the fact that the parameter space allowed by the *cold dark matter* (CDM) requirements turns out [18, 19] to lie lower than the one allowed by the inclusive decay $b \rightarrow s\gamma$ in the $m_{\text{LSP}} - \Delta_{\tilde{\tau}_2}$ plane, where m_{LSP} is the mass of the lightest sparticle (LSP), which, in our case, is the lightest neutralino $\tilde{\chi}$ and $\Delta_{\tilde{\tau}_2} = (m_{\tilde{\tau}_2} - m_{\text{LSP}})/m_{\text{LSP}}$ is the relative mass splitting between the LSP and the lightest stau mass eigenstate $\tilde{\tau}_2$. This result is strengthened by the fact that $\mu < 0$ is strongly disfavored by the constraint arising from the deviation δa_μ of the measured value of the muon anomalous magnetic moment a_μ from its predicted value a_μ^{SM} in the *standard model* (SM). Indeed, $\mu < 0$ is defended only at 3σ by the calculation of a_μ^{SM} based on the τ -decay data, whereas there is a stronger and stronger tendency at present to prefer the e^+e^- -annihilation data for the calculation of a_μ^{SM} , which favor the $\mu > 0$ regime. Given the above situation, we

*Electronic address: nikar@auth.gr

†Electronic address: lazaride@eng.auth.gr

‡Electronic address: kpallis@auth.gr

focus here on the $\mu > 0$ case.

Let us recall that, in this case, the suitable ‘asymptotic’ Yukawa quasi-unification condition applied [16, 19] is

$$h_t : h_b : h_\tau = |1 + c| : |1 - c| : |1 + 3c|. \quad (1)$$

This relation depends on a single parameter c , which is taken, for simplicity, to be real and lying in the range $0 < c < 1$. With fixed masses for the fermions of the third generation, we can determine the parameters c and $\tan\beta$ so that Eq. (1) is satisfied. In contrast to the original version of the CMSSM [2–4], therefore, $\tan\beta$ is not a free parameter but it can be restricted, within our set-up, via Eq. (1) to relatively large values. The remaining free parameters of our model are the universal soft SUSY breaking parameters defined at M_{GUT} , i.e.,

$$M_{1/2}, \quad m_0, \quad \text{and} \quad A_0, \quad (2)$$

where the symbols above denote the common gaugino mass, scalar mass, and trilinear scalar coupling constant, respectively. These parameters can be restricted by employing a number of experimental and cosmological requirements as in Refs. [16, 19]. In view of the expected data from the *Large Hadron Collider* (LHC), it would be worth to retest our model against observations using the most up-to-date version of the available constraints.

We exhibit the cosmological and phenomenological requirements which we considered in our investigation in Sec. II and we restrict the parameter space of our model in Sec. III. Finally, we test our model from the perspective of the CDM direct detection experiments in Sec. IV and summarize our conclusions in Sec. V.

II. COSMOLOGICAL AND PHENOMENOLOGICAL CONSTRAINTS

In our investigation, we integrate the two-loop renormalization group equations for the gauge and Yukawa coupling constants and the one-loop ones for the soft SUSY breaking parameters between M_{GUT} and a common SUSY threshold $M_{\text{SUSY}} \simeq (m_{\tilde{t}_1} m_{\tilde{t}_2})^{1/2}$ ($\tilde{t}_{1,2}$ are the stop mass eigenstates) determined in consistency with the SUSY spectrum. At M_{SUSY} , we impose radiative electroweak symmetry breaking, evaluate the SUSY spectrum employing the publicly available calculator **SOFTSUSY** [20], and incorporate the SUSY corrections to the b and τ mass [12]. The corrections to the τ -lepton mass m_τ (almost 4%) lead [16, 18] to a small decrease of $\tan\beta$. From M_{SUSY} to M_Z , the running of gauge and Yukawa coupling constants is continued using the SM renormalization group equations.

The parameter space of our model can be restricted by using a number of phenomenological and cosmological constraints. We calculate them using the latest version of the publicly available code **micrOMEGAS** [21]. We now briefly discuss these requirements – for similar recent analyses, see Ref. [22] for CMSSM or Refs. [14, 23] for MSSM with YU.

a. SM Fermion Masses. The masses of the fermions of the third generation play a crucial role in the determination of the evolution of the Yukawa coupling constants. For the b -quark mass, we adopt as an input parameter in our analysis the $\overline{\text{MS}}$ b -quark mass, which at 1σ is [24]

$$m_b(m_b)^{\overline{\text{MS}}} = 4.19_{-0.06}^{+0.18} \text{ GeV}. \quad (3)$$

This range is evolved up to M_Z using the central value $\alpha_s(M_Z) = 0.1184$ [24] of the strong fine structure constant at M_Z and then converted to the $\overline{\text{DR}}$ scheme in accordance with the analysis of Ref. [25]. We obtain, at 95% c.l.,

$$2.745 \lesssim m_b(M_Z)/\text{GeV} \lesssim 3.13 \quad (4)$$

with the central value being $m_b(M_Z) = 2.84 \text{ GeV}$. For the top-quark mass, we use the central pole mass (M_t) as an input parameter [26]:

$$M_t = 173 \text{ GeV} \Rightarrow m_t(m_t) = 164.6 \text{ GeV} \quad (5)$$

with $m_t(m_t)$ being the running mass of the t quark. We also take the central value $m_\tau(M_Z) = 1.748 \text{ GeV}$ [25] of the $\overline{\text{DR}}$ tau-lepton mass at M_Z .

b. Cold Dark Matter Considerations. According to the WMAP results [27], the 95% c.l. range for the CDM abundance is

$$\Omega_{\text{CDM}} h^2 = 0.1126 \pm 0.0072. \quad (6)$$

In the context of the CMSSM, the LSP can be the lightest neutralino $\tilde{\chi}$ and naturally arises as a CDM candidate. We require its relic abundance $\Omega_{\text{LSP}} h^2$ in the universe not to exceed the upper bound derived from Eq. (6) – the lower bound is not considered since other production mechanisms [28] of LSPs may be present too and/or other CDM candidates [29, 30] may also contribute to $\Omega_{\text{CDM}} h^2$. So, at 95% c.l., we take

$$\Omega_{\text{LSP}} h^2 \lesssim 0.12. \quad (7)$$

An upper bound on m_{LSP} (or $m_{\tilde{\chi}}$) can be derived from Eq. (7) since, in general, $\Omega_{\text{LSP}} h^2$ increases with m_{LSP} . The calculation of $\Omega_{\text{LSP}} h^2$ in **micrOMEGAS** includes accurately thermally averaged exact tree-level cross sections of all the possible (co)annihilation processes [3, 31], treats poles [4, 16, 32] properly, and uses one-loop QCD and SUSY QCD corrections [11, 16, 33, 34] to the Higgs decay widths and couplings to fermions.

c. The Branching Ratio $\text{BR}(b \rightarrow s\gamma)$ of $b \rightarrow s\gamma$. The most recent experimental world average for $\text{BR}(b \rightarrow s\gamma)$ is known [35] to be $(3.52 \pm 0.23 \pm 0.09) \times 10^{-4}$ and its updated SM prediction is $(3.15 \pm 0.23) \times 10^{-4}$ [36]. Combining in quadrature the experimental and theoretical errors involved, we obtain the following constraints on this branching ratio at 95% c.l.:

$$2.84 \times 10^{-4} \lesssim \text{BR}(b \rightarrow s\gamma) \lesssim 4.2 \times 10^{-4}. \quad (8)$$

The computation of $\text{BR}(b \rightarrow s\gamma)$ in the `micrOMEGAs` package presented in Ref. [34] includes [37] *next-to-leading order* (NLO) QCD corrections to the charged Higgs boson (H^\pm) contribution, the $\tan\beta$ enhanced contributions, and resummed NLO SUSY QCD corrections. The H^\pm contribution interferes constructively with the SM contribution, whereas the SUSY contribution interferes destructively with the other two contributions for $\mu > 0$. The SM plus the H^\pm and SUSY contributions initially increases with m_{LSP} and yields a lower bound on m_{LSP} from the lower bound in Eq. (8). (For higher values of m_{LSP} , it starts mildly decreasing.)

d. *The Branching Ratio* $\text{BR}(B_s \rightarrow \mu^+\mu^-)$ of $B_s \rightarrow \mu^+\mu^-$. The rare decay $B_s \rightarrow \mu^+\mu^-$ occurs via Z penguin and box diagrams in the SM and, thus, its branching ratio is highly suppressed. The SUSY contribution, though, originating [38, 39] from neutral Higgs bosons in chargino-, H^\pm -, and W^\pm -mediated penguins behaves as $\tan^6\beta/m_A^4$ and hence is particularly important for large $\tan\beta$'s. We impose the following 95% c.l. upper bound:

$$\text{BR}(B_s \rightarrow \mu^+\mu^-) \lesssim 5.8 \times 10^{-8} \quad (9)$$

as reported [40] by the CDF collaboration. This bound implies a lower bound on m_{LSP} since $\text{BR}(B_s \rightarrow \mu^+\mu^-)$ decreases as m_{LSP} increases.

e. *The Branching Ratio* $\text{BR}(B_u \rightarrow \tau\nu)$ of $B_u \rightarrow \tau\nu$. The purely leptonic decay $B_u \rightarrow \tau\nu$ proceeds via W^\pm - and H^\pm -mediated annihilation processes. The SUSY contribution, contrary to the SM one, is not helicity suppressed and depends on the mass m_{H^\pm} of the charged Higgs boson since it behaves [39, 41] as $\tan^4\beta/m_{H^\pm}^4$. The ratio $R(B_u \rightarrow \tau\nu)$ of the CMSSM to the SM branching ratio of $B_u \rightarrow \tau\nu$ increases with m_{LSP} and approaches unity. It is to be consistent with the following 95% c.l. range [35]:

$$0.52 \lesssim R(B_u \rightarrow \tau\nu) \lesssim 2.04. \quad (10)$$

A lower bound on m_{LSP} can be derived from the lower bound in this inequality.

f. *Muon Anomalous Magnetic Moment*. The quantity δa_μ , which is defined in Sec. I, can be attributed to SUSY contributions arising from chargino-sneutrino and neutralino-smuon loops. The relevant calculation is based on the formulas of Ref. [42]. The absolute value of the result decreases as m_{LSP} increases and its sign is positive for $\mu > 0$. On the other hand, the calculation of a_μ^{SM} is not yet stabilized mainly because of the ambiguities in the calculation of the hadronic vacuum-polarization contribution. According to the most up-to-date evaluation of this contribution in Ref. [43], there is still a discrepancy between the findings based on the e^+e^- -annihilation data and the ones based on the τ -decay data. Taking into account the more reliable calculation based on the e^+e^- data and the experimental measurements [44] of a_μ , we obtain the following 95% c.l. range:

$$12.7 \times 10^{-10} \lesssim \delta a_\mu \lesssim 44.7 \times 10^{-10}. \quad (11)$$

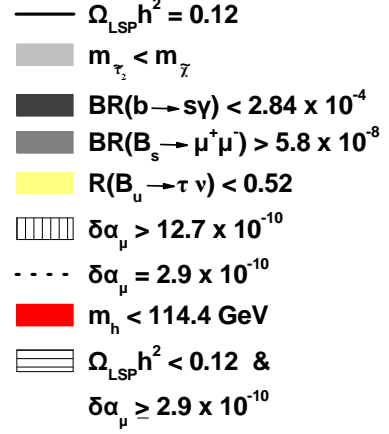


FIG. 1: Summary of the conventions adopted in Figs. 2 and 3 for the various restrictions on the parameters of the model.

The τ -decay based calculation, on the other hand, yields the following 95% c.l. range:

$$2.9 \times 10^{-10} \lesssim \delta a_\mu \lesssim 36.1 \times 10^{-10}. \quad (12)$$

A lower [upper] bound on m_{LSP} can be derived from the upper [lower] bound in Eqs. (11) and (12). As it turns out, only the upper bound on m_{LSP} is relevant in our case. Taking into account the aforementioned computational instabilities, we will impose the less stringent upper bound on m_{LSP} from the τ -decay based calculation. However, we will also depict the more stringent bound from the e^+e^- -annihilation data for comparison.

g. *Collider Bounds*. For our analysis, the only relevant collider bound is the 95% c.l. LEP bound [45] on the lightest CP-even neutral Higgs boson mass

$$m_h \gtrsim 114.4 \text{ GeV}, \quad (13)$$

which gives a lower bound on m_{LSP} . The calculation of m_h in the package `SOFTSUSY` [20] includes the full one-loop SUSY corrections and some zero-momentum two-loop corrections [46]. The results are well tested [47] against other spectrum calculators.

III. RESTRICTIONS ON THE SUSY PARAMETERS

Imposing the requirements described above, we can delineate the allowed parameter space of our model. The predicted mass spectra are possibly relevant for the LHC searches. Throughout our investigation, we consider the central values for the SM parameters M_t , $m_b(M_Z)$, $m_\tau(M_Z)$, and $\alpha_s(M_Z)$. We adopt the following conventions for the various lines and regions in the relevant figures (Figs. 2 and 3) – see Fig. 1:

- on the solid black line, Eq. (7) is saturated,

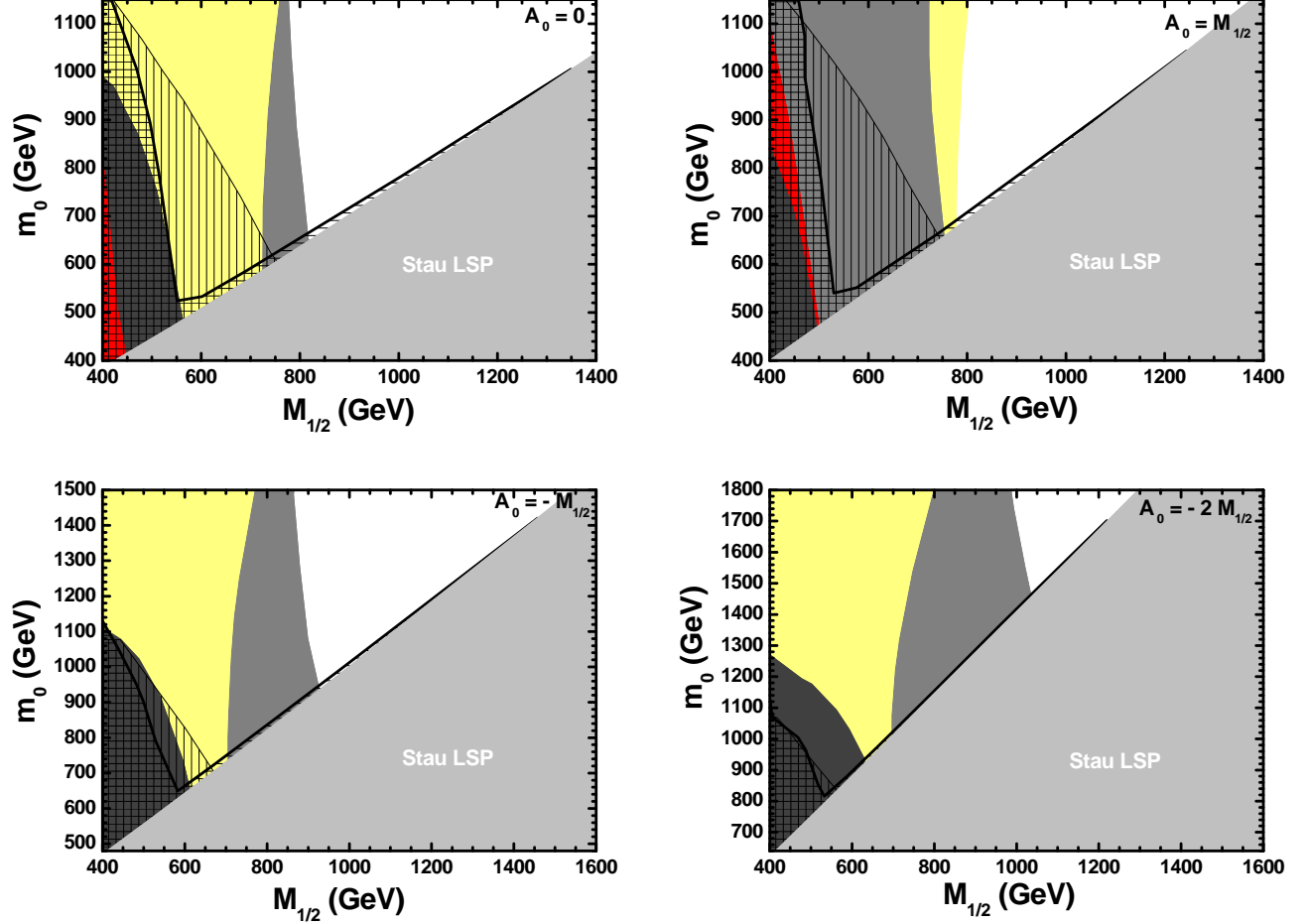


FIG. 2: Restrictions in the $M_{1/2} - m_0$ plane for various values of $A_0/M_{1/2}$ indicated in the graphs. The conventions adopted are described in Fig. 1.

- the light gray region is cosmologically excluded since it predicts charged LSP,
- the dark gray region is excluded by the lower bound in Eq. (8),
- the gray region is excluded by Eq. (9),
- the yellow region is excluded by the lower bound in Eq. (10),
- the vertically hatched region is favored by the lower bound in Eq. (11),
- on the dotted black line, the lower bound in Eq. (12) is saturated,
- the red region is excluded by Eq. (13),
- the horizontally hatched region is allowed by both Eq. (7) and the lower bound in Eq. (12).

Note that the upper bounds in Eqs. (8), (10), (11), and (12) do not restrict the parameters of our model.

We present the restrictions from all the requirements imposed in the $M_{1/2} - m_0$ plane for $A_0/M_{1/2} = 0, 1, -1$, and -2 in Fig. 2. We remark that the lower bound on $M_{1/2}$ comes from Eq. (9) for $A_0/M_{1/2} = 0, -1$, and -2 and from the lower bound in Eq. (10) for $A_0/M_{1/2} = 1$. Also, from the relevant data, we observe that the lower bound in Eq. (10) is fulfilled for the mass of the CP-odd Higgs boson $m_A \simeq 520$ GeV and almost independently of the other parameters. Finally, note that, for $A_0/M_{1/2} = -1$ and -2 , the bound in Eq. (13) is violated for $M_{1/2} < 400$ GeV and, consequently, does not appear in the relevant diagrams.

The constraint in Eq. (7) is, in general, satisfied in two well-defined distinct regions in the diagrams of Fig. 2. In particular,

- the region to the left of the almost vertical part of the line corresponding to the upper bound on $M_{1/2}$ from Eq. (7), where the LSP annihilation via the s -channel exchange of a CP-odd Higgs boson A is by far the dominant (co)annihilation process. However, this region is excluded by the constraints

in Eqs. (9) and (10). On the other hand, it is well known – see e.g. Refs. [4, 16] – that this region is extremely sensitive to variations of $m_b(M_Z)$. Indeed, we find that as $m_b(M_Z)$ decreases, the A -boson mass m_A increases and approaches $2m_{\text{LSP}}$. The A -pole neutralino annihilation is then enhanced and $\Omega_{\text{LSP}}h^2$ is drastically reduced causing an increase of the upper bound on $M_{1/2}$. However, even if we reduce $m_b(M_Z)$, we do not find any A -pole annihilation region which is allowed by the requirements of Eqs. (9) and (10).

- the narrow region which lies just above the light gray area with charged LSP, where bino-stau coannihilations [3, 31] take over leading to a very pronounced reduction of $\Omega_{\text{LSP}}h^2$. A large portion of this region survives after the application of the requirements in Eqs. (9) and (10) and constitutes the overall allowed parameter range of our model for the given A_0 . To get a better understanding of this area, we can replace the parameter m_0 by the relative mass splitting $\Delta\tilde{\tau}_2$ between the LSP and the lightest stau, defined in Sec. I. We observe that the overall allowed region requires $\Delta\tilde{\tau}_2 \lesssim 0.025$. It is evident from Fig. 2 that the slope of the boundary line with $\Delta\tilde{\tau}_2 = 0$ increases as $A_0/M_{1/2}$ moves away from zero in both directions. Note that this slope in our model turns out to be larger than the one obtained in other versions of the CMSSM – cf. Ref. [3] – with lower values of $\tan\beta$. As a consequence, small variations of m_0 or $M_{1/2}$ lead, in our model, to more drastic variations in $\Delta\tilde{\tau}_2$.

Finally, we note that the more stringent upper bound on $M_{1/2}$ from the lower bound in Eq. (11) is not satisfied for the values taken for $A_0/M_{1/2}$ in Fig. 2, with the values $A_0/M_{1/2} = 0$ and 1 being much more favored. On the other hand, the lower bound in Eq. (12) is fulfilled in the whole allowed region for $A_0/M_{1/2} = 0$ and 1 whereas, for $A_0/M_{1/2} = -1$ and -2 , it imposes an upper bound on $M_{1/2}$ which overshadows the bound on $M_{1/2}$ from Eq. (7). Since the saturation of the lower bound in Eq. (12) occurs for $\Delta\tilde{\tau}_2 \lesssim 0.01$, the portion of the dotted black line – see Fig. 1 – which connects the black solid line with the boundary of the gray area is not visible in the relevant panels of Fig. 2.

To get a better idea of the allowed parameter space, we focus on the coannihilation regime and construct the allowed region in the $M_{1/2} - A_0/M_{1/2}$ plane. This is shown in Fig. 3, where we depict the restrictions on the parameters from the various constraints for $\Delta\tilde{\tau}_2 = 0$. This choice ensures the maximal possible reduction of $\Omega_{\text{LSP}}h^2$ due to the $\tilde{\chi} - \tilde{\tau}_2$ coannihilation. So, for $\Delta\tilde{\tau}_2 = 0$, we find the maximal $M_{1/2}$ or m_{LSP} allowed by Eq. (7) for a given value of $A_0/M_{1/2}$. We observe that, for $-0.8 \lesssim A_0/M_{1/2} \lesssim 3$ [$-2.55 \lesssim A_0/M_{1/2} \lesssim -0.8$ and $3 \lesssim A_0/M_{1/2} \lesssim 3.21$] the overall upper bound on $M_{1/2}$ or m_{LSP} is derived from the bound in Eq. (7) [lower bound in Eq. (12)]. We find that, for $A_0/M_{1/2} < 0$, processes

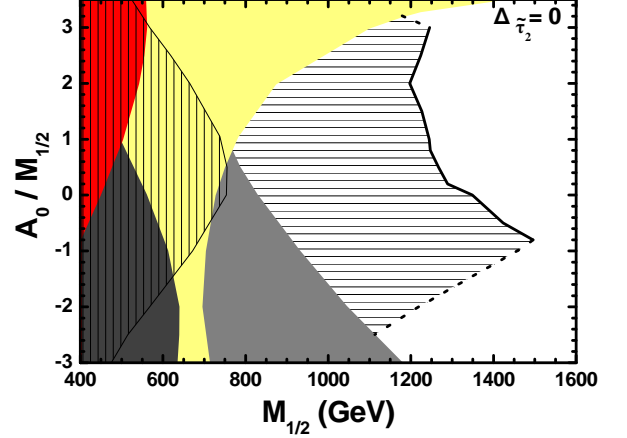


FIG. 3: Restrictions in the $M_{1/2} - A_0/M_{1/2}$ plane for $\Delta\tilde{\tau}_2 = 0$ following the conventions of Fig. 1, but with the horizontally hatched region not extended to areas excluded by other constraints.

with $\tilde{\tau}_2\tilde{\tau}_2^*$ in the initial state and $W^\pm W^\mp$, $W^\pm H^\mp$ in the final one become more efficient (with a total contribution to the effective cross section of about 14 to 21% as $A_0/M_{1/2}$ decreases from 0 to -2.55) and so coannihilation is strengthened and m_{LSP} 's larger than in the $A_0/M_{1/2} > 0$ case are allowed. The overall maximal $M_{1/2} \simeq 1495.4$ GeV or $m_{\text{LSP}} \simeq 677$ GeV is encountered at $A_0/M_{1/2} \simeq -0.8$. On the other hand, for $-2.55 \lesssim A_0/M_{1/2} \lesssim 0.7$ [$0.7 \lesssim A_0/M_{1/2} \lesssim 3.21$] the lower bound on $M_{1/2}$ or m_{LSP} is derived from the bound in Eq. (9) [lower bound in Eq. (10)]. The overall allowed lowest $M_{1/2} \simeq 771.22$ GeV or $m_{\text{LSP}} \simeq 341$ GeV is encountered at $A_0/M_{1/2} \simeq 0.7$. Let us remark that the more stringent upper bound on $M_{1/2}$ from the lower bound in Eq. (11) is not satisfied in the allowed region of our model, since there is no common region between the horizontally and the vertically hatched areas for any $A_0/M_{1/2}$. However, for $0 \lesssim A_0/M_{1/2} \lesssim 1$, these areas are quite close to each other. Note that increasing $\Delta\tilde{\tau}_2$ within its allowed range $0 - 0.025$ does not alter the boundaries of the various constraints in any essential way, except the solid line which is displaced to the left so that the allowed area shrinks considerably.

The deviation from YU can be estimated by defining [19] the relative splittings δh_b and δh_τ at M_{GUT} through the relations:

$$\delta h_b \equiv \frac{h_b - h_t}{h_t} = -\frac{2c}{1+c} = -\delta h_\tau \equiv \frac{h_t - h_\tau}{h_t}. \quad (14)$$

In the allowed (horizontally hatched) area of Fig. 3, the ranges of the parameters c , δh_τ , δh_b , and $\tan\beta$ are

$$\begin{aligned} 0.149 &\lesssim c \lesssim 0.168, \\ 0.26 &\lesssim \delta h_\tau = -\delta h_b \lesssim 0.29, \\ 56.3 &\lesssim \tan\beta \lesssim 57.7. \end{aligned} \quad (15)$$

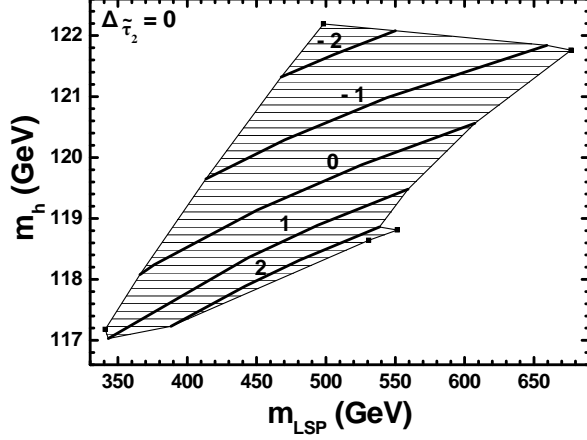


FIG. 4: The allowed (horizontally hatched) region in the $m_{\text{LSP}} - m_h$ plane for $\Delta\tilde{\tau}_2 \simeq 0$. We also depict the curves corresponding to various values of $A_0/M_{1/2}$, indicated on them. The dark points on the boundary correspond to $A_0/M_{1/2} = -2.55, -0.8, 3, 3.21$, and 0.8 starting from the point at the top of the allowed area and moving clockwise.

Let us underline that, although the required deviation from YU is not so small, the restrictions from YU are not completely lost since $\tan\beta$ remains large – close to 60 – and the deviation from YU is generated in a GUT-inspired well-motivated way.

Taking into account the results depicted in Fig. 3, we can make predictions for the sparticle and the Higgs boson spectrum of our model, which may be observable at the LHC. In Table I, we list the model input and output parameters, the masses in GeV of the sparticles – neutralinos $\tilde{\chi}$, $\tilde{\chi}_2^0$, $\tilde{\chi}_3^0$, $\tilde{\chi}_4^0$, charginos $\tilde{\chi}_1^\pm$, $\tilde{\chi}_2^\pm$, gluinos \tilde{g} , squarks \tilde{t}_1 , \tilde{t}_2 , \tilde{b}_1 , \tilde{b}_2 , \tilde{u}_L , \tilde{u}_R , \tilde{d}_L , \tilde{d}_R , and sleptons $\tilde{\tau}_1$, $\tilde{\tau}_2$, $\tilde{\nu}_\tau$, \tilde{e}_L , \tilde{e}_R , $\tilde{\nu}_e$ – and the Higgs bosons (h , H , H^\pm , A), and the values of the various low energy observables for $A_0/M_{1/2} = 0, \pm 1$, and -2 and for the lowest possible $M_{1/2}$ in each case adjusting $\Delta\tilde{\tau}_2$ so as $\Omega_{\text{LSP}} h^2 \simeq 0.11$. Note that we consider the squarks and sleptons of the two first generations as degenerate. From the values of the various observable quantities, it is easy to verify that all the relevant constraints are met. We also included in Table I predictions for the possible direct detection of the LSP using central values for the hadronic inputs f_{Tq}^p or Δ_q^p – see Sec. IV.

For the lowest masses of the Higgs and sparticle spectrum (m_h and m_{LSP}), we present even more explicit predictions in Fig. 4, where we depict the allowed m_h 's versus m_{LSP} for $\Delta\tilde{\tau}_2 \simeq 0$ and $A_0/M_{1/2} = 0, \pm 1$, and ± 2 . As can be seen from Fig. 3, the lower limits on the solid lines for $A_0/M_{1/2} = 0, -1$, and -2 [$A_0/M_{1/2} = 1$ and 2] are found from the bound in Eq. (9) [lower bound in Eq. (10)] – see also Table I. On the other hand, the upper limits of the solid lines for $A_0/M_{1/2} = 0, 1$, and 2 [$A_0/M_{1/2} = -1$ and -2] are found from the bound in Eq. (7) [lower bound in Eq. (12)]. The approximate overall allowed area in the

TABLE I: Input and output parameters, masses of the sparticles and Higgs bosons, and values of the low energy observables of our model for four values of $A_0/M_{1/2}$. Recall that $1 \text{ pb} \simeq 2.6 \times 10^{-9} \text{ GeV}^{-2}$.

Input parameters				
$A_0/M_{1/2}$	0	1	-1	-2
c	0.161	156	0.165	0.168
$M_{1/2}/\text{GeV}$	825.7	776.06	927.25	1041.8
m_0/GeV	665.4	687.5	943.1	1466.8
Output parameters				
$\tan\beta$	57	56.8	57.4	57.7
$h_t(M_{\text{GUT}})$	0.58	0.58	0.58	0.58
$100\delta h_\tau(M_{\text{GUT}})$	27.7	26.9	28.3	28.7
μ/GeV	925.8	804	1170	1505
$\Delta\tilde{\tau}_2(\%)$	2.46	2.45	2.13	1.52
Masses in GeV of sparticles and Higgs bosons				
$\tilde{\chi}$	365.7	342.7	413.2	467.5
$\tilde{\chi}_2^0$	705	656	802	909
$\tilde{\chi}_3^0$	927	807	1170	1502
$\tilde{\chi}_4^0$	940	827	1177	1506
$\tilde{\chi}_1^\pm$	940	827	1177	1506
$\tilde{\chi}_2^\pm$	705	656	802	909
\tilde{g}	1916	1813	2145	2412
\tilde{t}_1	1585	1530	1752	1980
\tilde{t}_2	1383	1352	1506	1666
\tilde{b}_1	1578	1526	1752	2008
\tilde{b}_2	1498	1454	1670	1916
\tilde{u}_L	1052	1762	2134	2585
\tilde{u}_R	1011	1694	2054	2503
\tilde{d}_L	1055	1764	2135	2586
\tilde{d}_R	1006	1764	2045	2494
$\tilde{\tau}_1$	777	754	956	1283
$\tilde{\tau}_2$	374.7	351.1	422	474.6
$\tilde{\nu}_\tau$	756	738	939	1272
\tilde{e}_L	880	875	1142	1635
\tilde{e}_R	740	752	1010	1523
$\tilde{\nu}_e$	876	871	1139	1633
h	118.1	117	119.7	121.3
H	584	519	668	747.6
H^\pm	591	527	674	752.8
A	585	520	669	748
Low energy observables				
$10^4 \text{BR}(b \rightarrow s\gamma)$	3.32	3.41	3.32	3.37
$10^8 \text{BR}(B_s \rightarrow \mu^+ \mu^-)$	5.76	5.3	5.78	5.8
$\text{R}(B_u \rightarrow \tau\nu)$	0.61	0.52	0.69	0.74
$10^{10} \delta a_\mu$	10.6	11.6	6.9	3.9
$\Omega_{\text{LSP}} h^2$	0.11	0.11	0.11	0.11
$\sigma_{\tilde{\chi}p}^{\text{SI}}/10^{-9} \text{pb}$	0.536	1.1	0.2	0.076
$\sigma_{\tilde{\chi}p}^{\text{SD}}/10^{-7} \text{pb}$	1.96	4.1	0.6	0.2

$m_{\text{LSP}} - m_h$ plane is hatched. Shown are also the boundary points of this region at $A_0/M_{1/2} \simeq -2.55, -0.8, 3, 3.21$, and 0.7 starting from the point at the top of the allowed area and moving clockwise.

As one can see from Fig. 4, m_h increases with m_{LSP} and as A_0 decreases. Since the maximum allowed m_{LSP} from the bound in Eq. (7) or the lower bound in Eq. (12) is achieved at $\Delta\tilde{\tau}_2 \simeq 0$ for given A_0 , we conclude that the maximum possible allowed m_h can be obtained for $\Delta\tilde{\tau}_2 \simeq 0$. On the other hand, the minimum possible allowed m_h practically coincides with its value for $\Delta\tilde{\tau}_2 \simeq 0$ since variation of $\Delta\tilde{\tau}_2$ within the values allowed by Eq. (7) causes minor modifications of m_h for fixed $M_{1/2}$. For $A_0 = 0$, we find $826.4 \lesssim M_{1/2}/\text{GeV} \lesssim 1348.9$ or $365.9 \lesssim m_{\text{LSP}}/\text{GeV} \lesssim 607.4$ and $118.1 \lesssim m_h/\text{GeV} \lesssim 120.6$. The overall minimum [maximum] m_h is 117.03 [122.2] obtained at $A_0/M_{1/2} \simeq 1$ [$A_0/M_{1/2} \simeq -2.55$] for $M_{1/2} = 776.6$ GeV [$M_{1/2} = 1106.6$ GeV] or $m_{\text{LSP}} \simeq 343.1$ GeV [$m_{\text{LSP}} \simeq 498.3$ GeV].

IV. CDM DIRECT DETECTION

As we have shown, our model possesses a limited and well-defined range of parameters allowed by all the relevant cosmological and phenomenological constraints. It would be, thus, interesting to investigate whether the predicted LSPs in the universe could be detected in the current or planned direct CDM searches [48–50], which look for evidence of weakly-interacting massive particles through scattering on nuclei. The quantities which are conventionally used in the recent literature for comparing experimental results and theoretical predictions are the spin-independent (SI) and spin-dependent (SD) lightest neutralino-proton ($\tilde{\chi} - p$) scattering cross sections $\sigma_{\tilde{\chi}p}^{\text{SI}}$ and $\sigma_{\tilde{\chi}p}^{\text{SD}}$, respectively.

These quantities are calculated by employing the relevant routine of the `micrOMEGAs` package [51] based on the full one-loop treatment of Ref. [52], which happens to agree with the tree-level approximation [53] for the values of the SUSY parameters encountered in our model. Following the approach of Refs. [51, 53], we calculate the scalar form factors for light quarks in the proton f_{Tq}^p (with $q = u, d, s$), needed for the calculation of $\sigma_{\tilde{\chi}p}^{\text{SI}}$, via the formulas:

$$f_{Td}^p = \frac{2\sigma_{\pi N}}{m_p \left(1 + \frac{m_u}{m_d}\right) \left(1 + \frac{B_u}{B_d}\right)}, \quad (16a)$$

$$f_{Tu}^p = \frac{m_u}{m_d} \frac{B_u}{B_d} f_{Td}^p, \quad (16b)$$

$$f_{Ts}^p = \frac{y\sigma_{\pi N}}{m_p \left(1 + \frac{m_u}{m_d}\right)} \frac{m_s}{m_d}. \quad (16c)$$

Here we take for the mass of the proton $m_p = 0.939$ GeV and for the light quark mass ratios

$$\frac{m_u}{m_d} = 0.553 \pm 0.043 \quad \text{and} \quad \frac{m_s}{m_d} = 18.9 \pm 0.8, \quad (17)$$

whereas the ratio B_u/B_d is evaluated from

$$\frac{B_u}{B_d} = \frac{2z - (z-1)y}{2 + (z-1)y} \quad (18)$$

with $z = 1.49$. The uncertainties in z and the quark mass ratios are negligible compared to the uncertainties in the pion-nucleon sigma term $\sigma_{\pi N}$ and the fractional strange quark content of the nucleon y , for which recent lattice simulations suggest [54] that, at 68% c.l.,

$$\sigma_{\pi N} = 53_{-7.3}^{+21.1} \text{ MeV} \quad \text{and} \quad y = 0.030_{-0.018}^{+0.017}. \quad (19)$$

Taking into account the relations above, we find the following 1σ ranges for the f_{Tq}^p 's:

$$f_{Tu}^p = 0.024_{-0.0032}^{+0.0095}, \quad (20a)$$

$$f_{Td}^p = 0.029_{-0.0042}^{+0.012}, \quad (20b)$$

$$f_{Ts}^p = 0.021_{-0.013}^{+0.025}. \quad (20c)$$

Note that f_{Ts}^p turns out to be considerably smaller than its older value – cf. Ref. [19] – reducing thereby the extracted $\sigma_{\tilde{\chi}p}^{\text{SI}}$.

For the calculation of $\sigma_{\tilde{\chi}p}^{\text{SD}}$, the relevant axial-vector form factors for light quarks in the proton Δ_q^p (with $q = u, d, s$) are taken to lie in their 1σ ranges [55]:

$$\Delta_u^p = +0.842 \pm 0.012, \quad (21a)$$

$$\Delta_d^p = -0.427 \pm 0.013, \quad (21b)$$

$$\Delta_s^p = -0.085 \pm 0.018. \quad (21c)$$

Taking the central value of $\Omega_{\text{LSP}} h^2$ in Eq. (6), but allowing the hadronic inputs f_{Tq}^p or Δ_q^p to vary within their ranges in Eqs. (20a)-(20c) or (21a)-(21c), respectively, we derive the dark gray, gray, and light gray hatched bands in the $m_{\text{LSP}} - \sigma_{\tilde{\chi}p}^{\text{SI}}$ or $m_{\text{LSP}} - \sigma_{\tilde{\chi}p}^{\text{SD}}$ plane corresponding to $A_0/M_{1/2} = 0, 0.7$, and -0.8 , respectively – Fig. 5. The selected values of $A_0/M_{1/2}$ allow us to cover the whole range of the allowed m_{LSP} 's in our model – cf. Fig. 4. The bold solid lines in the middle of the bands of the left panel in Fig. 5 correspond to the central values of the f_{Tq}^p 's. We used the central value of $\Omega_{\text{LSP}} h^2$ since, as it turns out, for fixed m_{LSP} , $\sigma_{\tilde{\chi}p}^{\text{SI}}$ and $\sigma_{\tilde{\chi}p}^{\text{SD}}$ are almost insensitive to the variation of $\Omega_{\text{LSP}} h^2$ within the range of Eq. (6) – or, equivalently, to the required variation of $\Delta\tilde{\tau}_2$. The width of the bands is almost exclusively due to the variation of f_{Tq}^p or Δ_q^p . As a consequence, the bands in the $m_{\text{LSP}} - \sigma_{\tilde{\chi}p}^{\text{SI}}$ plane are wider than those in the $m_{\text{LSP}} - \sigma_{\tilde{\chi}p}^{\text{SD}}$ plane due to the larger uncertainties involved in the determination of the f_{Tq}^p 's. In the left panel of Fig. 5, we depict by a dashed green line the recently announced [49] upper bound on $\sigma_{\tilde{\chi}p}^{\text{SI}}$ from XENON which is slightly lower than the one from CDMSII [48], which is not included in the panel. We also draw with dotted red lines the projected sensitivities of SuperCDMS at Soudan and SNOLAB [56] – from top to bottom. Our model can be ultimately tested by XENON-1 ton, whose

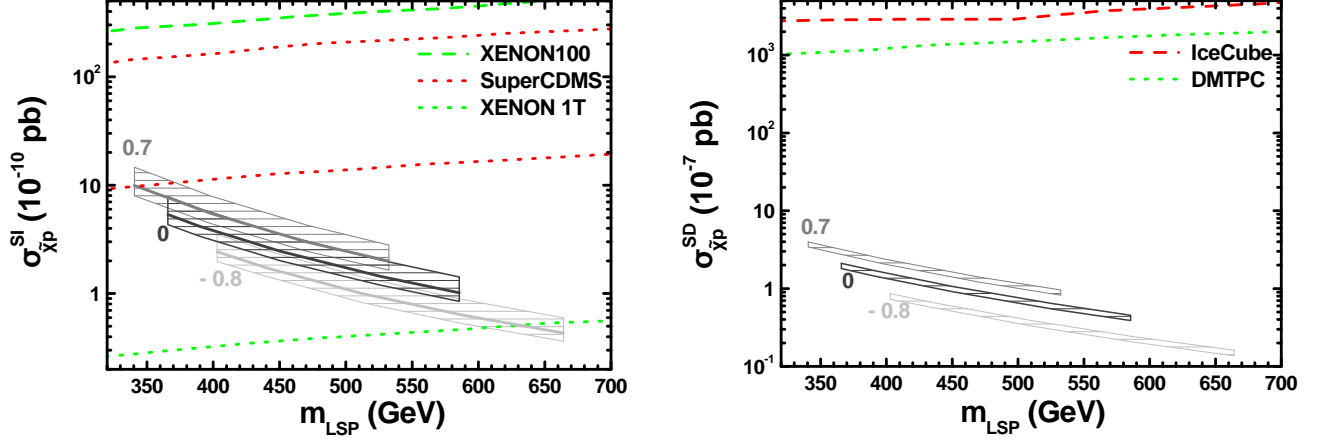


FIG. 5: The SI and SD $\tilde{\chi} - p$ cross sections $\sigma_{\tilde{\chi}p}^{\text{SI}}$ and $\sigma_{\tilde{\chi}p}^{\text{SD}}$, respectively, versus m_{LSP} for various $A_0/M_{1/2}$'s indicated in the graphs. The bold solid lines in the left panel are derived by fixing $\Omega_{\text{LSP}} h^2$ and f_{Tq}^p to their central values in Eqs. (6) and (20a)-(20c), whereas the hatched bands in both panels by allowing the hadronic inputs f_{Tq}^p or Δ_q^p to vary in their ranges in Eqs. (20a)-(20c) or (21a)-(21c). The present and planned sensitivity limits of the various experimental projects are also depicted by dashed and dotted lines, respectively.

planned sensitivity [56], depicted by a green dotted line, covers almost the whole available parameter space of the model. On the contrary, as can be easily deduced from the right panel of Fig. 5, $\sigma_{\tilde{\chi}p}^{\text{SD}}$ in our model lies well below the sensitivity of IceCube [50] (assuming neutralino annihilation into W^+W^-) – depicted by a dashed red line – and the expected limit from the large DMTPC detector [56], denoted by a dotted green line. Therefore, the LSPs predicted by our model can be detectable in the future projects which will release data on $\sigma_{\tilde{\chi}p}^{\text{SI}}$. Furthermore, the overall upper bound on m_{LSP} found in Sec. III – $m_{\text{LSP}} \lesssim 677$ GeV – implies lower bounds on $\sigma_{\tilde{\chi}p}^{\text{SI}}$ and $\sigma_{\tilde{\chi}p}^{\text{SD}}$. Namely,

$$\sigma_{\tilde{\chi}p}^{\text{SI}} \gtrsim 4.3 \text{ (3.6)} \times 10^{-11} \text{ pb and } \sigma_{\tilde{\chi}p}^{\text{SD}} \gtrsim 1.5 \text{ (1.4)} \times 10^{-8} \text{ pb,} \quad (22)$$

where the bounds in parentheses are derived by allowing the f_{Tq}^p 's and Δ_q^p 's to vary within 1σ . Needless to say that the low values of $\sigma_{\tilde{\chi}p}^{\text{SI}}$ and $\sigma_{\tilde{\chi}p}^{\text{SD}}$ obtained here are due to the fact that we use universal ‘asymptotic’ gaugino masses and, thus, the LSP is an almost pure bino, as in every version of the CMSSM.

V. CONCLUSIONS

We performed a revised scan of the parameter space of the CMSSM with $\mu > 0$ applying a suitable Yukawa quasi-unification condition predicted by the SUSY GUT model of Ref. [16], which has been constructed in order to remedy the b -quark mass problem arising from exact Yukawa unification and universal boundary conditions. We took into account updated constraints from collider and cosmological data. These constraints originate from

the CDM abundance in the universe, B physics ($b \rightarrow s\gamma$, $B_s \rightarrow \mu^+\mu^-$, and $B_u \rightarrow \tau\nu$), $\delta\alpha_\mu$, and m_h . We showed that our model possesses a limited but not unnaturally small range of parameters which is consistent with all these requirements. Namely, the constraint arising from CDM considerations can be satisfied simultaneously with all the other constraints thanks to the drastic reduction of the LSP relic density by neutralino-stau coannihilations. For $A_0 = 0$, we find $365.9 \lesssim m_{\text{LSP}}/\text{GeV} \lesssim 607.4$ and $118.1 \lesssim m_h/\text{GeV} \lesssim 120.6$, whereas, in the overall allowed region of our model, we have $-2.55 \lesssim A_0/M_{1/2} \lesssim 3.21$ with $341 \lesssim m_{\text{LSP}}/\text{GeV} \lesssim 677$ and $117 \lesssim m_h/\text{GeV} \lesssim 122.2$. Almost all the allowed parameter space of our model will be accessible in future CDM direct experiments which look for SI cross sections between neutralino and proton.

It is worth mentioning that the present investigation constitutes an improved version of the analysis in Ref. [16]. The consideration of the constraints from $\text{BR}(B_s \rightarrow \mu^+\mu^-)$ and $R(B_u \rightarrow \tau\nu)$, the updated experimental results for all the other constraints, and the evaluation of the particle spectrum employing SOFTSUSY are the main improvements in this work. The results obtained are significantly different from the previous ones.

Note Added

While this work was under completion, we became aware of Ref. [57], where the CMSSM with Yukawa quasi-unification is also analyzed. Although our results as regards $\tan\beta$, c , $\sigma_{\tilde{\chi}p}^{\text{SI}}$, and $\sigma_{\tilde{\chi}p}^{\text{SD}}$ are similar, there are large discrepancies as regards the CMSSM mass parameters and, consequently, the mass spectrum. In particular,

the ratio $(m_A - 2m_{\text{LSP}})/2m_{\text{LSP}}$, which determines the strength of the A -pole effect in reducing $\Omega_{\text{LSP}}h^2$, is not allowed to be lower than 0.2 in our case and, thus, this effect is excluded. Indeed, the portion of the parameter space allowed by Eq. (7) due to A -pole neutralino annihilations is excluded by the B -physics constraints in our analysis – contrary to the findings of Ref. [57]. These discrepancies can be possibly attributed to the fact that we use different numerical routines for the calculation of both the SUSY spectra and the low energy observables. It is well known [58] that the predictions of the various SUSY spectrum calculators do not coincide in the large $\tan\beta$ regime. Our results as regards the implementation of the electroweak symmetry breaking are consistent with our initial investigation in Ref. [16].

Acknowledgments

We would like to thank G. Bélanger, M.E. Gómez, S. Heinemeyer, A. Pukhov, and P. Slavich for enlightening correspondence as well as I. Gogoladze and Q. Shafi for useful discussions related to Ref. [57]. This work was supported by the European Union under the Marie Curie Initial Training Network ‘UNILHC’ PITN-GA-2009-237920 and also by the European Union (European Social Fund - ESF) and Greek national funds through the Operational Program ‘Education and Lifelong Learning’ of the National Strategic Reference Framework (NSRF) - Research Funding Program: Heracleitus II. Investing in knowledge society through the European Social Fund.

-
- [1] R. Arnowitt, A. Chamseddine and P. Nath, Phys. Rev. Lett. **49**, 970 (1982); R. Arnowitt, A. Chamseddine and P. Nath, Nucl. Phys. **B227**, 121 (1983); L.J. Hall, J.D. Lykken and S. Weinberg, Phys. Rev. **D27**, 2359 (1983).
 - [2] R. Arnowitt and P. Nath, Phys. Rev. Lett. **69**, 725 (1992); G.G. Ross and R.G. Roberts, Nucl. Phys. **B377**, 571 (1992); V.D. Barger, M.S. Berger and P. Ohmann, Phys. Rev. D **49**, 4908 (1994); G.L. Kane, C. Kolda, L. Roszkowski and J.D. Wells, Phys. Rev. D **49**, 6173 (1994).
 - [3] J.R. Ellis, T. Falk, and K.A. Olive, Phys. Lett. B **444**, 367 (1998); J.R. Ellis, T. Falk, K.A. Olive, and M. Srednicki, Astropart. Phys. **13**, 181 (2000); **15**, 413(E) (2001).
 - [4] A.B. Lahanas, D.V. Nanopoulos, and V.C. Spanos, Phys. Rev. D **62**, 023515 (2000); J.R. Ellis, T. Falk, G. Gani, K.A. Olive, and M. Srednicki, Phys. Lett. B **510**, 236 (2001).
 - [5] G. Lazarides and C. Panagiotakopoulos, Phys. Lett. B **337**, 90 (1994); S. Khalil, G. Lazarides, and C. Pallis, *ibid.* **508**, 327 (2001).
 - [6] B. Ananthanarayan, G. Lazarides, and Q. Shafi, Phys. Rev. D **44**, 1613 (1991); Phys. Lett. B **300**, 245 (1993).
 - [7] I. Antoniadis and G.K. Leontaris, Phys. Lett. B **216**, 333 (1989).
 - [8] R. Jeannerot, S. Khalil, G. Lazarides, and Q. Shafi, J. High Energy Phys. **10**, 012 (2000).
 - [9] H. Baer, M.A. Diaz, J. Ferrandis, and X. Tata, Phys. Rev. D **61**, 111701 (2000); H. Baer, M. Brhlik, M.A. Diaz, J. Ferrandis, P. Mercadante, P. Quintana, and X. Tata, *ibid.* **63**, 015007 (2000); D. Auto, H. Baer, C. Balázs, A. Belyaev, J. Ferrandis, and X. Tata, J. High Energy Phys. **06**, 023 (2003); D. Auto, H. Baer, A. Belyaev, and T. Krupovnickas, *ibid.* **10**, 066 (2004).
 - [10] T. Blažek, R. Dermíšek, and S. Raby, Phys. Rev. Lett. **88**, 111804 (2002); Phys. Rev. D **65**, 115004 (2002); R. Dermíšek, S. Raby, L. Roszkowski, and R. Ruiz de Austri, J. High Energy Phys. **04**, 037 (2003).
 - [11] M.S. Carena, M. Olechowski, S. Pokorski, and C.E.M. Wagner, Nucl. Phys. **B426**, 269 (1994); R. Hempfling, Phys. Rev. D **49**, 6168 (1994); L.J. Hall, R. Rattazzi, and U. Sarid, *ibid.* **50**, 7048 (1994).
 - [12] D.M. Pierce, J.A. Bagger, K.T. Matchev, and R. Zhang, Nucl. Phys. **B491**, 3 (1997); M.S. Carena, D. Garcia, U. Nierste, and C.E.M. Wagner, *ibid.* **B577**, 88 (2000).
 - [13] P.Z. Skands *et al.*, J. High Energy Phys. **07**, 036 (2004).
 - [14] S.F. King and M. Oliveira, Phys. Rev. D **63**, 015010 (2001); I. Gogoladze, R. Khalid, S. Raza, and Q. Shafi, arXiv:1008.2765 [hep-ph]; I. Gogoladze, R. Khalid, and Q. Shafi, Phys. Rev. D **79**, 115004 (2009); **80**, 095016 (2009).
 - [15] U. Chattopadhyay and P. Nath, Phys. Rev. D **65**, 075009 (2002); U. Chattopadhyay, A. Corsetti, and P. Nath, *ibid.* **66**, 035003 (2002); C. Pallis, Nucl. Phys. **B678**, 398 (2004).
 - [16] M.E. Gómez, G. Lazarides, and C. Pallis, Nucl. Phys. **B638**, 165 (2002).
 - [17] R. Jeannerot, S. Khalil, and G. Lazarides, J. High Energy Phys. **07**, 069 (2002); G. Lazarides and A. Vamvasakis, Phys. Rev. D **76**, 083507 (2007); **76**, 123514 (2007); G. Lazarides, I.N.R. Peddie, and A. Vamvasakis, *ibid.* **78**, 043518 (2008); G. Lazarides, arXiv:1006.3636.
 - [18] M.E. Gómez, G. Lazarides, and C. Pallis, Phys. Rev. D **67**, 097701 (2003).
 - [19] G. Lazarides and C. Pallis, hep-ph/0404266; hep-ph/0406081.
 - [20] B.C. Allanach, Computer Physics Commun. **143**, 305 (2002).
 - [21] G. Belanger, F. Boudjema, A. Pukhov, and A. Semenov, <http://lapth.in2p3.fr/micromegas>; G. Belanger, F. Boudjema, P. Brun, A. Pukhov, S. Rosier-Lees, P. Salati, and A. Semenov, Comput. Phys. Commun. **182**, 842 (2011).
 - [22] R. Trotta, F. Feroz, M.P. Hobson, L. Roszkowski, and R. Ruiz de Austri, J. High Energy Phys. **12**, 024 (2008); A. Belyaev, S. Dar, I. Gogoladze, A. Mustafayev, and Q. Shafi, arXiv:0712.1049 [hep-ph]; O. Buchmueller *et al.*, Eur. Phys. J. C **64**, 391 (2009); Y. Akrami, P. Scott, J. Edsjo, J. Conrad, and L. Bergstrom, J. High Energy Phys. **04**, 057 (2010); L. Roszkowski, R. Ruiz de Austri, and R. Trotta, Phys. Rev. D **82**, 055003 (2010).
 - [23] H. Baer, S. Kraml, S. Sekmen, and H. Summy, J. High Energy Phys. **03**, 056 (2008); **10**, 079 (2008); H. Baer, S. Kraml, and S. Sekmen, *ibid.* **09**, 005 (2009); H. Baer, S. Kraml, A. Lessa, and S. Sekmen, *ibid.* **02**, 055 (2010); H. Baer, S. Kraml, A. Lessa, S. Sekmen, and H. Summy,

- Phys. Lett. B **685**, 72 (2010).
- [24] K. Nakamura *et al.* [Particle Data Group], J. Phys. G **37**, 075021 (2010).
 - [25] H. Baer, J. Ferrandis, K. Melnikov, and X. Tata, Phys. Rev. D **66**, 074007 (2002); K. Tobe and J.D. Wells, Nucl. Phys. B **663**, 123 (2003).
 - [26] Tevatron Electroweak Working Group (CDF and D0 collaborations), arXiv:0903.2503; T. Aaltonen *et al.* [CDF Collaboration], Phys. Rev. Lett. **105**, 252001 (2010).
 - [27] E. Komatsu *et al.* [WMAP Collaboration], Astrophys. J. Suppl. **192**, 18 (2011); <http://lambda.gsfc.nasa.gov/product/map>.
 - [28] N. Fornengo, A. Riotto, and S. Scopel, Phys. Rev. D **67**, 023514 (2003); C. Pallis, Astropart. Phys. **21**, 689 (2004); J. Cosmol. Astropart. Phys. **10**, 015 (2005); Nucl. Phys. B **751**, 129 (2006); hep-ph/0610433.
 - [29] J.R. Ellis, K.A. Olive, Y. Santoso, and V.C. Spanos, Phys. Lett. B **588**, 7 (2004); L. Covi, L. Roszkowski, R. Ruiz de Austri, and M. Small, J. High Energy Phys. **06**, 003 (2004).
 - [30] H. Baer and H. Summy, Phys. Lett. B **666**, 5 (2008); H. Baer, M. Haider, S. Kraml, S. Sekmen, and H. Summy, J. Cosmol. Astropart. Phys. **02**, 002 (2009).
 - [31] M.E. Gómez, G. Lazarides, and C. Pallis, Phys. Rev. D **61**, 123512 (2000); Phys. Lett. B **487**, 313 (2000).
 - [32] T. Nihei, L. Roszkowski, and R. Ruiz de Austri, J. High Energy Phys. **05**, 063 (2001); **07**, 024 (2002).
 - [33] C. Pallis and M.E. Gómez, hep-ph/0303098.
 - [34] G. Bélanger, F. Boudjema, A. Pukhov, and A. Semenov, Comput. Phys. Commun. **174**, 577 (2006).
 - [35] E. Barberio *et al.* [Heavy Flavor Averaging Group], arXiv:0808.1297.
 - [36] M. Misiak *et al.*, Phys. Rev. Lett. **98**, 022002 (2007).
 - [37] M. Ciuchini, G. Degrossi, P. Gambino, and G.F. Giudice, Nucl. Phys. B **527**, 21 (1998); F. Borzumati and C. Greub, Phys. Rev. D **58**, 074004 (1998); G. Degrossi, P. Gambino, and G.F. Giudice, J. High Energy Phys. **12**, 009 (2000); M.E. Gómez, T. Ibrahim, P. Nath, and S. Skadhauge, Phys. Rev. D **74**, 015015 (2006).
 - [38] P.H. Chankowski and L. Slawianowska, Phys. Rev. D **63**, 054012 (2001); C.S. Huang, W. Liao, Q.S. Yan, and S.H. Zhu, *ibid.* **63**, 114021 (2001); **64**, 059902(E) (2001); C. Bobeth, T. Ewerth, F. Kruger, and J. Urban, *ibid.* **64**, 074014 (2001); A. Dedes, H.K. Dreiner, and U. Nierste, Phys. Rev. Lett. **87**, 251804 (2001); J.R. Ellis, K.A. Olive, and V.C. Spanos, Phys. Lett. B **624**, 47 (2005).
 - [39] F. Mahmoudi, Comput. Phys. Commun. **180**, 1579 (2009).
 - [40] T. Aaltonen *et al.* [CDF Collaboration], Phys. Rev. Lett. **100**, 101802 (2008).
 - [41] G. Isidori and P. Paradisi, Phys. Lett. B **639**, 499 (2006); G. Isidori, F. Mescia, P. Paradisi and D. Temes, Phys. Rev. D **75**, 115019 (2007).
 - [42] S.P. Martin and J.D. Wells, Phys. Rev. D **64**, 035003 (2001).
 - [43] M. Davier, A. Hoecker, B. Malaescu, and Z. Zhang, Eur. Phys. J. C **71**, 1515 (2011).
 - [44] G.W. Bennett *et al.* [Muon $g - 2$ Collaboration], Phys. Rev. D **73**, 072003 (2006).
 - [45] The LEP Collaborations ALEPH, DELPHI, L3, OPAL, The LEP Working Group for Higgs Boson Searches, Eur. Phys. J. C **47**, 547 (2006).
 - [46] G. Degrossi, P. Slavich, and F. Zwirner, Nucl. Phys. B **611**, 403 (2001); A. Brignole, G. Degrossi, P. Slavich, and F. Zwirner, *ibid.* **B631**, 195 (2002); A. Brignole, G. Degrossi, P. Slavich, and F. Zwirner, *ibid.* **B643**, 79 (2002); A. Dedes, G. Degrossi, and P. Slavich, *ibid.* **B672**, 144 (2003).
 - [47] B.C. Allanach, S. Kraml, and W. Porod, J. High Energy Phys. **03**, 045 (2003); B.C. Allanach, A. Djouadi, J.L. Kneur, W. Porod, and P. Slavich, *ibid.* **09**, 044 (2004).
 - [48] Z. Ahmed *et al.* [CDMS-II Collaboration], Science **327**, 1619 (2010); Phys. Rev. Lett. **106**, 131302 (2011).
 - [49] E. Aprile *et al.* [XENON100 Collaboration], arXiv:1104.2549.
 - [50] R. Abbasi *et al.* [ICECUBE Collaboration], Phys. Rev. Lett. **102**, 201302 (2009).
 - [51] G. Belanger, F. Boudjema, A. Pukhov, and A. Semenov, Comput. Phys. Commun. **180**, 747 (2009).
 - [52] M. Drees and M. Nojiri, Phys. Rev. D **48**, 3483 (1993); G. Jungman, M. Kamionkowski, and K. Griest, Phys. Rep. **267**, 195 (1996).
 - [53] J.R. Ellis, K.A. Olive, and C. Savage, Phys. Rev. D **77**, 065026 (2008); J.R. Ellis, K.A. Olive, and P. Sandick, New J. Phys. **11**, 105015 (2009).
 - [54] H. Ohki *et al.*, Phys. Rev. D **78**, 054502 (2008); D. Toussaint and W. Freeman, Phys. Rev. Lett. **103**, 122002 (2009); J. Giedt, A.W. Thomas, and R.D. Young, Phys. Rev. Lett. **103**, 201802 (2009).
 - [55] A. Airapetian *et al.* [HERMES Collaboration], Phys. Rev. D **75**, 012007 (2007).
 - [56] <http://dmtools.berkeley.edu/limitplots>, maintained by R. Gaijskell, V. Mandic, and J. Filippini.
 - [57] S. Dar, I. Gogoladze, Q. Shafi, and C.S. Un, arXiv:1105.5122.
 - [58] G. Belanger, S. Kraml, and A. Pukhov, Phys. Rev. D **72**, 015003 (2005); H. Baer, J. Ferrandis, S. Kraml, and W. Porod, *ibid.* **73**, 015010 (2006).